

A Numerical Study of Transport and Shot Noise at 2D Hopping

Yusuf A. Kinkhabwala, Viktor A. Sverdlov, Alexander N.

Korotkov and Konstantin K. Likharev

Department of Physics and Astronomy, Stony Brook University, Stony Brook, NY 11794-3800

Department of Electrical Engineering, University of California - Riverside, Riverside, CA 92521

A bstract. We have used modern supercomputer facilities to carry out extensive Monte Carlo simulations of 2D hopping (at negligible Coulomb interaction) in conductors with the completely random distribution of localized sites in both space and energy, within a broad range of the applied electric field E and temperature T , both within and beyond the variable-range hopping region. The calculated properties include not only dc current and statistics of localized site occupation and hop lengths, but also the current fluctuation spectrum. Within the calculation accuracy, the model does not exhibit $1=f$ noise, so that the low-frequency noise at low temperatures may be characterized by the Fano factor F . For sufficiently large samples, F scales with conductor length L as $(L_c=L)^{\alpha}$, where $\alpha = 0.76 - 0.08 < 1$, where parameter L_c is interpreted as the average percolation cluster length. At relatively low E , the electric field dependence of parameter L_c is compatible with the law $L_c \propto E^{-0.911}$ which follows from directed percolation theory arguments.

PACS numbers: 72.20.Ee, 72.20.Ht, 73.50.Td

1. Introduction

The theory of hopping transport in disordered conductors [1, 2, 3] at negligible Coulomb interaction is often perceived a well-established (if not completed) field, with recent research focused mostly on Coulomb effects. However, only relatively recently it was recognized that shot noise (see, e.g., Ref. [4]) is a very important characteristic of electron transport. In particular, the suppression of the current fluctuation density $S_I(f)$ at low frequencies, relative to its Schottky formula value $2e\hbar I_i$ (where hI_i is the dc current), is a necessary condition for the so-called quasi-continuous ("sub-electron") charge transfer [5].

Earlier calculations of shot noise at hopping through very short samples (e.g., across thin [6, 7]) and simple lattice models of long conductors in 1D [8] and 2D [9] have shown that such suppression may, indeed, take place. However, calculations for the more realistic case of disordered 2D conductors have been limited to just one particular value of electric field [9]. It seemed important to examine whether the law governing this suppression is really as general as it seemed. Such examination, carried out in this work, has become practical only after the development of a new, advanced method of spectral density calculation [10] in combination with the use of modern supercomputers. (The work reported below took close to a million processor-hours of CPU time.)

As a useful by-product of this effort, we have obtained accurate quantitative characterization of not only the dependence of the average current on both temperature T and electric field E , but also the statistics of localized site occupation and hop lengths, which give a useful additional insight to the physics of hopping transport.

2. Model

We have studied hopping in 2D rectangular ($L \times W$) samples with "open" boundary conditions on the interface with well-conducting electrodes [9] – see inset in Fig. 1. In the present study, we have concentrated on broad samples with width $W = L_c$, where L_c is the effective percolation cluster size (see below). The conductor is assumed to be "fully frustrated": the localized sites are randomly distributed over the sample area, and the corresponding electron eigenenergies $\epsilon_j^{(0)}$ are randomly distributed over a sufficiently broad energy band, so that the 2D density of states ρ is constant at all energies relevant for conduction. Electrons can hop from any site j to any other site k with the rate

$$q_{jk} = q_{jk} \exp \left(-\frac{r_{jk}}{a} \right); \quad (1)$$

where $r_{jk} = \sqrt{(x_j - x_k)^2 + (y_j - y_k)^2}$ is the site separation distance, and a is the localization radius [11]. Such exponential dependence on the hop length has been assumed in virtually all theoretical studies of hopping. However, in contrast to most other authors, we take Eq. (1) literally even at small distances $r_{jk} \ll a$; this range is important only at very high fields and/or temperatures where the average value of r_{jk}

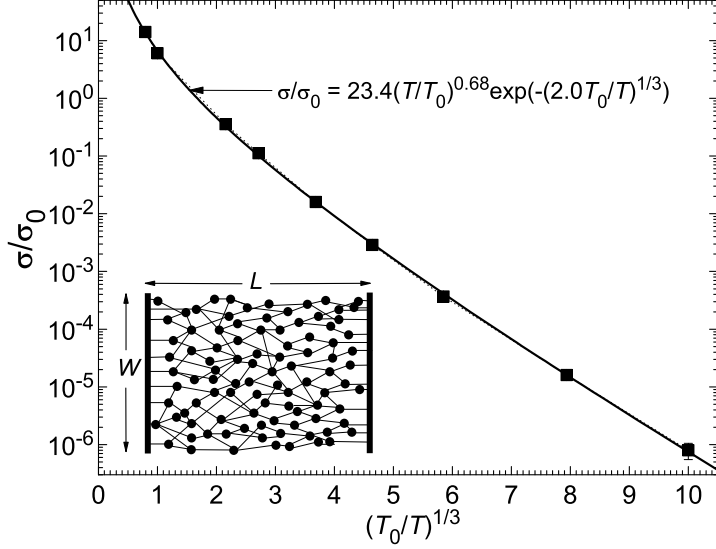


Figure 1. Linear conductivity σ as a function of temperature T . Points show the results of averaging over 80 samples varying in size ($L \times W$) from $(20 \times 10)\text{\AA}^2$ to $(160 \times 100)\text{\AA}^2$, biased by a low electric field $E = E_T$. Points are Monte Carlo results. The thin dashed line is just a guide for the eye, while the thick solid line corresponds to the best fit of the data by Eq. (5). Here and below, the error bars are smaller than the point size, unless they are shown explicitly. (The error bars correspond to the uncertainty in averaging over an ensemble of independent samples that is larger than the calculational uncertainty for each of the samples.) The inset shows the system under analysis (schematically).

becomes comparable to a . Of course our quantitative results for this particular region are only true for the localized states with exponential wavefunction decay.

Another distinction from some other works in this field is that we assume that the hopping rate amplitude U_{jk} depends continuously on the localized site energy difference $U_{jk} = U_j^{(0)} - U_k^{(0)} + eE r_{jk}$:

$$\sim_{jk} (U_{jk}) = g \frac{U_{jk}}{1 + \exp(-U_{jk}/k_B T)}: \quad (2)$$

This model coincides, for low phonon energies U_{jk} , with that described by Eqs. (4.2.17)–(4.2.19) of Ref. [2] for hopping in lightly-doped semiconductors, and of course satisfies the Gibbs detailed balance requirement $U_{jk} = U_{kj} \exp(-U_{jk}/k_B T)$. It is also closer, but more physical than the "Metropolis" dependence which has a cusp at $U_{jk} = 0$.

The interaction of hopping electrons is assumed negligible (with the exception of their implicit on-site interaction which forbids hopping into already occupied localized states). This assumption is well-justified for practically important materials, in particular amorphous silicon, which is the major candidate material for the

implementation of sub-electron charge transfer components in single-electronic circuits [12]. Indeed, the relative strength of the Coulomb interaction may be characterized by a dimensionless parameter $(\epsilon = a) / (\pi^2 \rho)$, where ρ is the 3D density of states near the Fermi level, and ϵ the relative dielectric constant. For undoped amorphous Si, ρ is of the order of $10^{16} \text{ eV}^{-1} \text{cm}^{-3}$, and only special treatments may increase it to $10^{20} \text{ eV}^{-1} \text{cm}^{-3}$ - see, e.g., Ref. [13]. With $\epsilon = 10$ and a of the order of a few nanometers (typical for the midgap states in Si), ϵ is much less than unity for the entire range of ϵ cited above, so that there is a broad range ($(\ln T)$; $(\ln E)$; $3 \ln (1/\epsilon)$) of temperature T and electric field E where the Coulomb interaction is negligible [4].

With this assumption, our model has only three energy scales: $k_B T$, eEa , and $(\epsilon_0 a^2)^{1/3}$. In other words, there are two characteristic values of electric field:

$$E_T = \frac{k_B T}{ea} \text{ and } E_0 = \frac{1}{\epsilon_0 a^3}; \quad (3)$$

We will be mostly interested in the case of low temperatures $T < T_0$, where

$$T_0 = \frac{1}{k_B \epsilon_0 a^2} \quad (4)$$

is the field-independent scale of temperature, so that the field scales are related as $E_T < E_0$. (The only role of the dimensionless parameter g introduced by Eq. (2) is to give the scale of hopping conductivity $\sigma_0 = g(\epsilon \approx 1)$. Coherent quantum effects leading to weak localization and metal-to-insulator transition are negligibly small, and hence the formulated hopping model is adequate, only if $g \approx 1$.)

The dynamic Monte Carlo calculations were carried out using the algorithm suggested by Bakhvalov et al. [15], which has become the de facto standard for the simulation of incoherent single-electron tunneling [16]. All calculated variables were averaged over the sample, and in most cases, over several (many) samples with independent random distributions of localized sites in space and energy, but with the same dimensionless parameters $L=a$, $W=a$, $T=T_0$, and $E=E_0$. We have used a new, advanced technique [10] of the noise (current spectral density) calculation to save simulation time. The used supercomputer facilities are listed in the Acknowledgments section below.

3. DC Current

In order to understand the relation between our model and the prior results in this field, we have started from the calculation of dc current hIi as a function of T and E . If the electric field is sufficiently small ($E \ll E_T$), then the current is proportional to E , and the transport is completely characterized by the linear conductivity $\sigma = hIi/W = E$. Fig. 1 shows the calculated conductivity as a function of temperature T . In the region $T < T_0$ this dependence follows the exponential T dependence of the 2D Mott law [1, 2, 3]

$$-\frac{1}{0} \frac{A(T;0) \exp \left(-B(T;0) \frac{T_0}{T} \right)^{1/3}}{T}; \quad (5)$$

where $A(T;E)$ and $B(T;E)$ are dimensionless, model-dependent slow functions of their arguments. We have found that our results may be well fit by Eq. 5) with the following pre-exponential function: $A(T;0) = (23.4 \pm 1.4) (T=T_0)^{0.68 \pm 0.04}$, and constant $B(T;0) = 2.0 \pm 0.2$. This latter result may be compared with the following values reported in the literature. In Ref. [17], B was analytically estimated to be close to 2.1. A different value, 3.45 ± 0.2 has been found by mapping a random 2D hopping problem to the problem of percolation in a system of linked spheres [18, 2]. Finally, a close value 3.25 (with no uncertainty reported) has been obtained using numerical simulations of hopping on a periodic lattice, with a slightly different model for the function (U) [19]. The difference between our result and the two last values is probably due to the differences between details of the used models.

At higher electric fields ($E \gg E_0$), dc current starts to grow faster than the Ohm law, so that if we still keep the above definition of conductivity, it starts to grow with E (Fig. 2). At $T = 0$, the results are well-described by the expression [22, 23, 24, 25, 26]

$$-\frac{d}{dE} \left[A(0;E) \exp \left(B(0;E) \frac{E_0}{E} \right) \right] = \dots \quad (6)$$

The data for not very high fields ($E \gg E_0$) may be well fit by Eq. 6) with constant $B(0;E) = 0.65 \pm 0.02$ and pre-exponential function $A(0;E) = (9.2 \pm 0.6) (E=E_0)^{0.80 \pm 0.02}$. (Note that the value $B(0;E) = 1.27$ given in Ref. [9] corresponds to a different pre-exponential function used for fitting.)

Finally, Fig. 2 shows that when the electric field becomes comparable with the value E_0 defined by the second of Eqs. 3), dc current and hence, conductivity, start to grow even faster than the exponential E dependence of Eq. (6).

4. Hopping Statistics

In order to understand the physics of hopping in the three field regions better, it is useful to have a look at the statistics of localized site occupation and hopping length. We have found that for all studied values of E and T , the probability of site occupation closely follows the Fermi distribution with the local Fermi level

$$\langle r \rangle = \frac{1}{L} \int_{-L/2}^{L/2} eE r \, dr \quad (7)$$

(where L is the Fermi level of the source electrode) and some effective temperature T_e . Points in Fig. 3 show T_e as a function of electric field E for several values of physical temperature T . Dashed lines show the result of the best fitting of the naive single-particle master equation

$$\frac{\partial f(r; t)}{\partial t} = \frac{Z}{d^2 r} \frac{d^0}{d^0 r} \exp \left(-\frac{r}{a} \right) f(r) \left[(1 + eE r) f(0) [1 - f(0)] + (1 - eE r) f(0) [1 - f(0)] g(0) \right] \quad (8)$$

by a stationary Fermi distribution. Equation (8) would follow from our model if electron correlation (in particular, percolation) effects were not substantial. In reality, we can

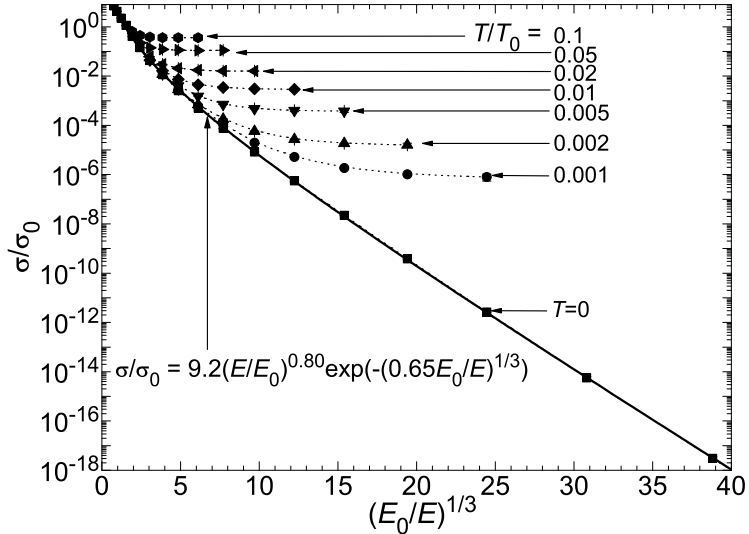


Figure 2. Nonlinear conductivity σ/σ_0 as a function of electric field E for several values of temperature T . Each point represents data averaged over 80 samples of the same size, ranging from $(20 \times 14)\text{Å}^2$ to $(1000 \times 700)\text{Å}^2$, depending on T and E . Points are Monte Carlo results. Thin dashed lines are only guides for the eye, while the thick solid line shows the best fit of the data by Eq. (6).

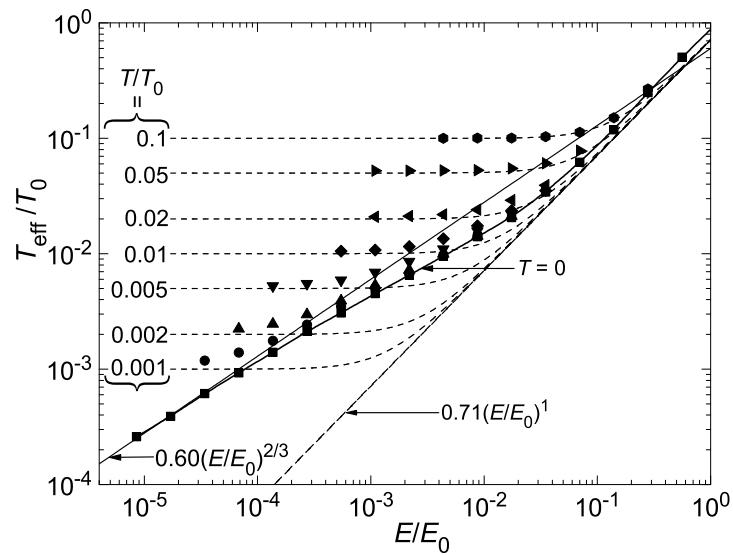


Figure 3. The effective temperature T_{eff} of current carriers as a function of electric field E for several values of temperature T . Closed points: Monte Carlo simulation results; dashed lines: master equation results. The solid curve marked $T = 0$ is only a guide for the eye.

expect the results following from Eq. (8) to be valid only in certain limits [20]. For example, in the low field limit $E \rightarrow 0$, both methods give $T_e = T$. At higher fields the effective temperature grows with the applied field, which "overheats" the electrons. At very high fields ($E = E_0 \approx 0.3$) both methods agree again and give

$$k_B T_e = C e E a; \quad C = 0.71 \quad 0.02; \quad (9)$$

(A similar result, but with $C = 1.34$, for our definition of a , was obtained by Marianer and Shklovskii [21] for a rather different model with an exponential energy dependence of the density of states.) However, at intermediate fields typical of "high-field" variable-range hopping ($E_T \leq E \leq E_0$), the master equation still gives the same result (9) and hence fails to appreciate that in fact T_e is proportional to $E^{2/3}$. In order to explain this result, let us discuss the statistics of hop lengths (Figs. 4 and 5).

The two- and one-dimensional histograms in Fig. 4 show the probability density P of a hop between two sites separated by the vector r , and also the density P_d weighed by the factor $\frac{1}{H_{jk}} H_{kj}$, where each H is the total number of hops (during a certain time interval) in the indicated direction, i.e. $jk \neq kj$. The latter weighting emphasizes the site pairs $(j;k)$ contributing substantially to the net hopping transport, in comparison with "blinking" pairs which exchange an electron many times before allowing it to advance along the field. It is clear that at relatively high temperatures or low fields ($E \ll E_T$) the non-weighed distribution should be symmetric (Fig. 4a). Figure 4d shows that in this case the one-dimensional probability density is well approximated by the Rayleigh distribution, $P(r) \propto r \exp(-r/a_e)$, with $a_e = a$. However, the weighed hop distribution is strongly asymmetric even in the limit $E \rightarrow 0$ (Fig. 4b). This asymmetry is even more evident at low temperatures or high fields ($E \gg E_T$); in this case the distribution has a sharp boundary (Fig. 4c). Figure 4d shows those cases where the 1D histograms deviate substantially from the distribution predicted by the master equation — see the first of Eqs. 16).

Figure 5 shows the results: non-weighed (r_{ms}) and direction-weighed (r_{mds}) hop lengths, defined, respectively, as

$$r_{ms}^2 = \frac{\int_0^\infty r_{jk}^2 P_{jk} dr_{jk}}{\int_0^\infty P_{jk} dr_{jk}} \quad (10)$$

and

$$r_{mds}^2 = \frac{\int_0^\infty r_{jk}^2 \frac{1}{H_{jk}} H_{kj} dr_{jk}}{\int_0^\infty \frac{1}{H_{jk}} H_{kj} dr_{jk}} \quad (11)$$

(that are of course just the averages of the histograms shown in Fig. 4), as functions of applied electric field for several values of temperature. At $T \rightarrow 0$, hopping is strictly one-directional (i.e., if $H_{jk} \neq 0$, then $H_{kj} = 0$), so that r_{ms} and r_{mds} are equal. In fact, simulation shows that in this limit both lengths coincide, at lower fields following the scaling [22]

$$r_{ms} = r_{mds} = D a \frac{E_0}{E}^{1/3}; \quad E_T \ll E \ll E_0; \quad (12)$$

with $D = 0.72 \pm 0.01$. (We are not aware of any prior results with which this value could be compared.)

This scaling of r in the variable-range hopping region is essentially the reason for the scaling of T_e mentioned above; in fact, the hopping electron gas "overheating" may be estimated by equating $k_B T_e$ to the energy gain $eE r_{\text{rms}}$, possibly multiplied by a constant of the order of one. For the effective temperature, this estimate gives

$$k_B T_e = \text{const} \quad eE r_{\text{rms}} = G e a E_0^{1/3} E^{2/3} = G \frac{(E = E_0)^{2/3}}{a^2}; \quad (13)$$

in accordance with the result shown in Fig. 3. Our Monte Carlo simulations give $G = 0.60 \pm 0.02$; we are not aware of any previous results with which this number could be compared.

At higher fields ($E \approx 0.1E_0$) the hop lengths start to decrease slower, approaching a few localization lengths a (Fig. 5a). In this ("ultra-high-field") region, the energy range $eE a$ for tunneling at distances of a few a is so high that there are always some accessible empty sites within this range, so that long hops, so dominant at variable-range hopping, do not contribute much into conduction.

At finite temperatures, the most curious result is a non-monotonic dependence of the rms hopping length on the applied field — see Fig. 5a. At $E \approx 0$, r_{rms} has to be field-independent, and there is no scale for it besides a . (As evident as it may seem, this fact is sometimes missed in popular descriptions of hopping.) In order to make a crude estimate of r_{rms} in this limit, one can use the master equation of Eq. (8). In this approach, at thermal equilibrium (i.e. at T independent of r), the hop length probability density $P(r)$ can be found as

$$P(r) = 2 \int_0^r d^3r' \exp \left[-\frac{r'}{a} \right] f^0(0) f(0) [1 - f^0(0)] + f^0(0) f(0) [1 - f^0(0)] g \left[\int_0^r d^3r' \exp \left[-\frac{r'}{a} \right] \right]; \quad (14)$$

in a good agreement with the results shown in Fig. 4d for this case. From Eq. (14), we get

$$r_{\text{rms}} = \sqrt{\frac{\int_0^R r^2 P(r) dr}{\int_0^R P(r) dr}} = \frac{R}{\sqrt{\frac{\int_0^R P(r) r^2 dr}{\int_0^R P(r) dr}}} = \frac{R}{\sqrt{\frac{P(0)}{P(R)}}} = 2.45a; \quad (15)$$

in a good agreement with numerical data shown in Fig. 5.

A similar calculation for r_{rms} may be obtained by expanding the tunneling rate $(\omega^0 + eE r)$ in small electric field as $(\omega^0 + eE r)^0 (\omega^0 + eE r)^1$. The result is

$$P_d(r) = eE r^2 \int_0^r d^3r' \exp \left[-\frac{r'}{a} \right] f^0(0) f^1(0) [1 - f^0(0)] + f^0(0) f^1(0) [1 - f^0(0)] g; \\ P_d(r) / r^2 \exp \left[-\frac{r}{a} \right];$$

$$r_{\text{m,ds}} = \frac{\int_0^R P_d(r) r^2 dr}{\int_0^R P_d(r) dr}^{1/2} = \frac{p}{12a} \quad 3.46a: \quad (16)$$

The Monte Carlo data (Fig. 5), however, differ from this result [7], showing that at $E = 0$, $r_{\text{m,ds}}$ obeys the Mott law [1, 2, 3]

$$r_{\text{m,ds}} = H a \left(\frac{T_0}{T} \right)^{1/3} + I a; \quad T = T_0; \quad (17)$$

with the best-fit values $H = 0.52 \pm 0.05$ and $I = 2.0 \pm 0.1$. In contrast, the function $r_{\text{m,s}}(T)$ is rather far from Eq. (17), because the Mott law refers to long hops responsible for transport (with the average approximately corresponding to $r_{\text{m,ds}}$), while $r_{\text{m,s}}$ reflects the statistics of all hops.

5. Shot Noise

The current noise simulation has been limited to the case of zero temperature for two reasons. First, in the opposite limit ($E_T = E$) current noise obeys the fluctuation-dissipation theorem; as a result, its low-frequency intensity can be found from $\langle T \rangle(T)$, and hence does not provide any new information. Second, the calculation of the spectral density $S_I(f)$ of current fluctuations with acceptable accuracy requires much larger statistical ensemble of random samples than that of the average current, which means it becomes increasingly difficult to extend it to finite temperatures even with the advanced averaging algorithm and substantial supercomputer resources used in this work.

Figure 6 shows a typical dependence of the current noise spectral density S_I , normalized to the Schottky value $2e\hbar I_i$, on the observation frequency $\omega = 2\pi f$. One can see a crossover from a low-frequency plateau to another plateau at high frequencies. As the sample length grows, the crossover becomes extended, i.e. features a broad intermediate range $\omega_1 \dots \omega_h$, just like in 1D systems with next-site hopping [8]. The position of the high-frequency end ω_h of this region can be estimated in the following way.

In all single-electron tunneling systems, the high-frequency plateau is reached at frequency ω_h close to the rate τ of the fastest electron hops affecting the total current [8, 9, 28, 29]. (For example, in systems described by the "orthodox" theory of single-electron tunneling, $\tau_{\text{max}} = U_{\text{max}} = e^2 R$, where R and C are, respectively, resistance and capacitance of a single junction [28, 29].) In our current case, this means that $\omega_h = (j_{\text{jk}})_{\text{max}} = (g=1) [U_{\text{jk}} \exp(-\tau_{\text{jk}}/a)]_{\text{max}}$. For this estimate, U_{jk} can be taken as $k_B T_e$ from Fig. 3, while according to the histograms shown in Fig. 4(d), the length of shortest hops, still giving a noticeable contribution to the current, can be estimated as $r_{\text{m,ds}} = 2$. For the case shown in Fig. 6 ($E = E_0 = 8.75 \times 10^3$), these estimates yield

$U_{\text{jk}} = k_B T_0 = 2 \times 10^2$, $(r_{\text{jk}})_{\text{min}} = a = 2.5$, giving finally $\tau = \tau_0 = 1.5 \times 10^3$, in a very reasonable agreement with numerical results shown in Fig. 6. (Note that this simple estimate, giving a length-independent value for τ_h , is only valid for relatively long and broad samples.)

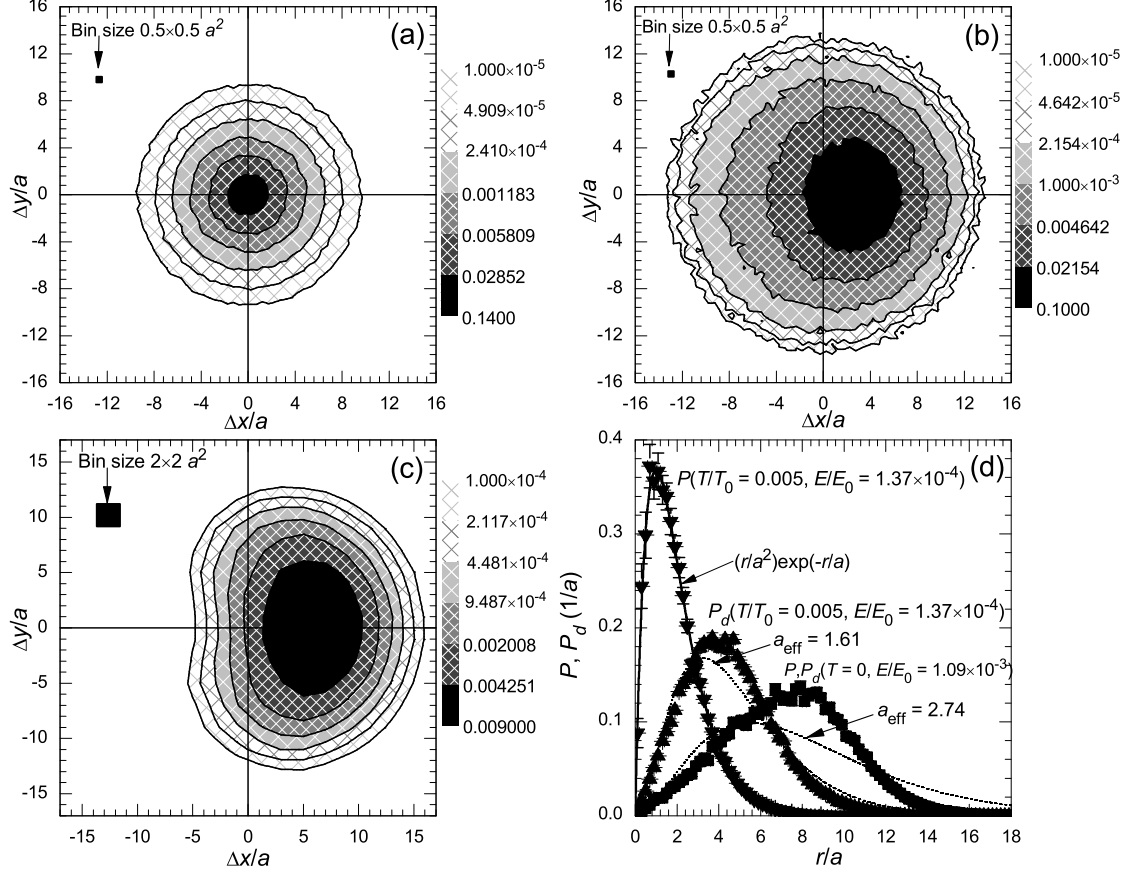


Figure 4. (a)–(c) Two-dimensional and (d) one-dimensional histograms of hop lengths for two typical cases: (a) and (b): $T = T_0 = 5 \times 10^{-3}$, $E = E_0 = 1.37 \times 10^{-4}$ ($E = E_T$) and (c): $T = 0$, $E = E_0 = 1.09 \times 10^{-3}$ ($E_T = E$). The shade-coding in panels (a) and (c) corresponds to the probability P of hops with given $r = (x; y)$, while that in panel (b), to the probability P_d weighed by factor $\prod_{jk} H_{jk} H_{kj} j$ —see the text. (Since at $T = 0$ there are no backward hops, for the case shown in panel (c), P and P_d coincide.) Panel (d) shows P and P_d , averaged over all directions of vector r , for the low-field, intermediate, and high-field cases. Dashed lines show the distribution (16) given by master equation, for the best-fit values of parameter a_{eff} .

At $T \neq 0$, a crossover to $1/f$ noise might be expected, because the discussion of this effect in some earlier publications [30, 31] was apparently independent of the Coulomb interaction between hopping electrons. However, within the accuracy of our simulations, we could not find any trace of $1/f$ -type noise for any parameters we have explored. This fact may not be very surprising, because all the discussions of the $1/f$ noise we are aware of require the presence of thermal fluctuations which are absent in our case ($T = 0$).

Since the low-frequency spectral density is flat, at $T = 0$ it may be considered as

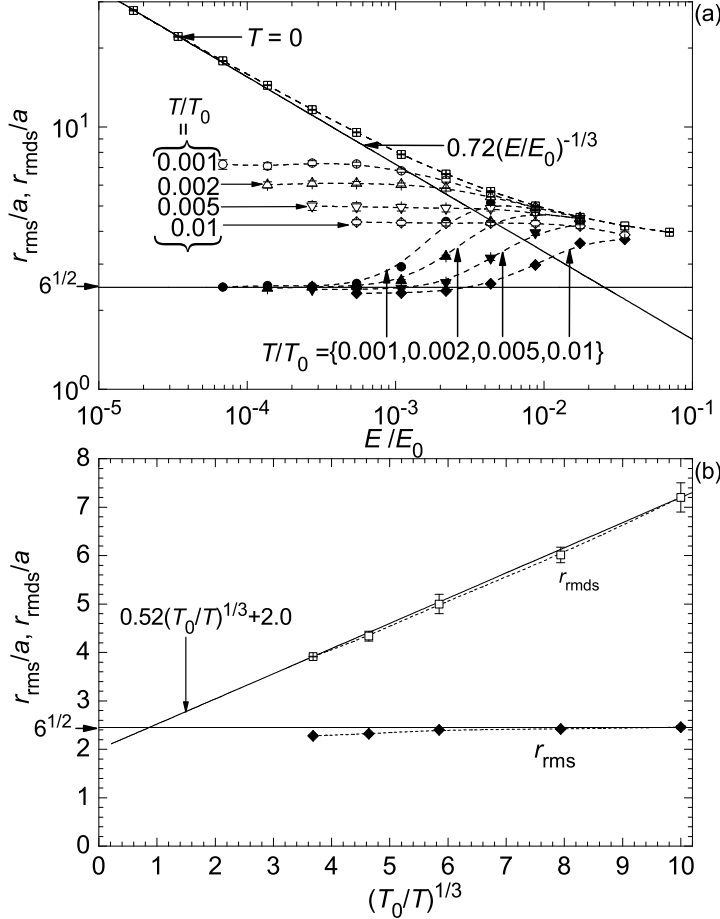


Figure 5. R M S. hop length r_{rms} (solid points) and the weighted average hop length r_{rmds} (open points) as functions: (a) of applied electric field E for several temperatures T , and (b) of temperature at $E = 0$. Tilted straight lines in panels (a) and (b) show the best fits by Eqs. (12) and (17), respectively, while the horizontal thin lines show the values following from the master equation. Curves are only guides for the eye.

shot noise [32] and characterized by the Fano factor [4]

$$F = \frac{S_I(f=0)}{2e\hbar I_i} : \quad (18)$$

Similarly, in order to characterize the shot noise at high-frequency spectral density, we may use the parameter

$$F_1 = \frac{S_I(f=1)}{2e\hbar I_i} : \quad (19)$$

Figure 7 (a) shows the average Fano factors F and F_1 as a function of L for several values of the applied electric field, while Fig. 7 (b) shows that the same data can be collapsed on universal curves by the introduction of certain length scales: L_c for F and L_h for F_1 .

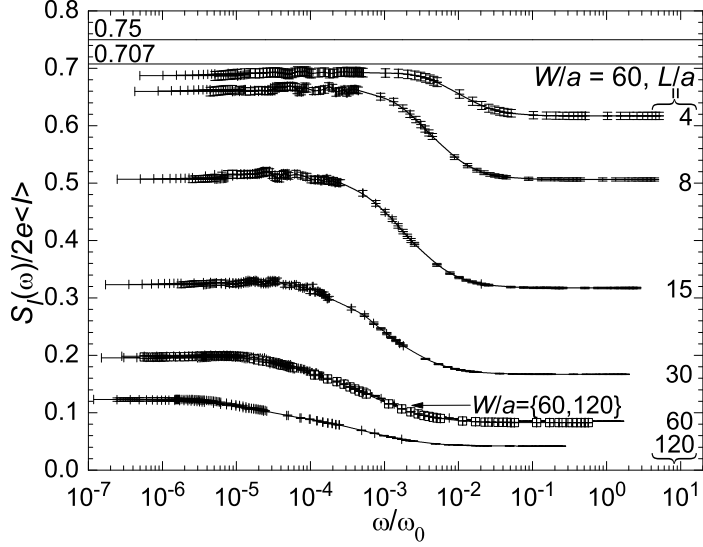


Figure 6. Spectral density S_I of current fluctuations normalized to the Schottky noise $2e\hbar I_i$ as a function of observation frequency ω , measured in units of ω_0 ($g \approx 0a^2$), for several values of sample length L for $T = 0$ and $E = E_0 = 8.75 \times 10^{-3}$. Small points show results for $W = a = 60$, while open squares are for $W = a = 120$ (at $L = a = 60$). Horizontal lines correspond to the Fano factor for hopping through short samples with one and two localized sites [6, 7]. Curves are only guides for the eye.

For the high frequency case,

$$F_1 = \frac{L_h}{L} ; \quad L \ll L_h; \quad (20)$$

where, within the accuracy of our calculations, $F_1 = 1$. Such dependence could be expected, because the high-frequency noise at hopping can be interpreted as a result of the 'capacitive division' of the discrete increments of externally measured charge jumps resulting from single-electron hops through the system [33]. When applied to uniform (ordered) systems, these arguments always give the result $F_1 = 1 = N_h$ with $N_h = L/d$ being the number of electron hops (d the hopping length along the current flow) necessary to pass an electron through the system, regardless of hop rates [4, 5, 8]. For $T \neq 0$ in the case of disordered conductors, L_h in Eq. (20) may then be interpreted as the average hop length along current flow. This interpretation turns out to be correct. Indeed, Fig. 8 shows that the parameter L_h obtained from Eq. (20) scales with the electric field in a manner similar to x_{rms} , especially at low fields, where it follows the variable-range hopping dependence of Eq. (12).

The low-frequency value F , in the limit ($L \ll L_c$), is weakly dependent on length and approaches $F = 0.7$, which not surprisingly is consistent with the prior results for hopping via 1 intermediate site [6] ($F = 0.75$) and 2 such sites [7] ($F = 0.707$). The

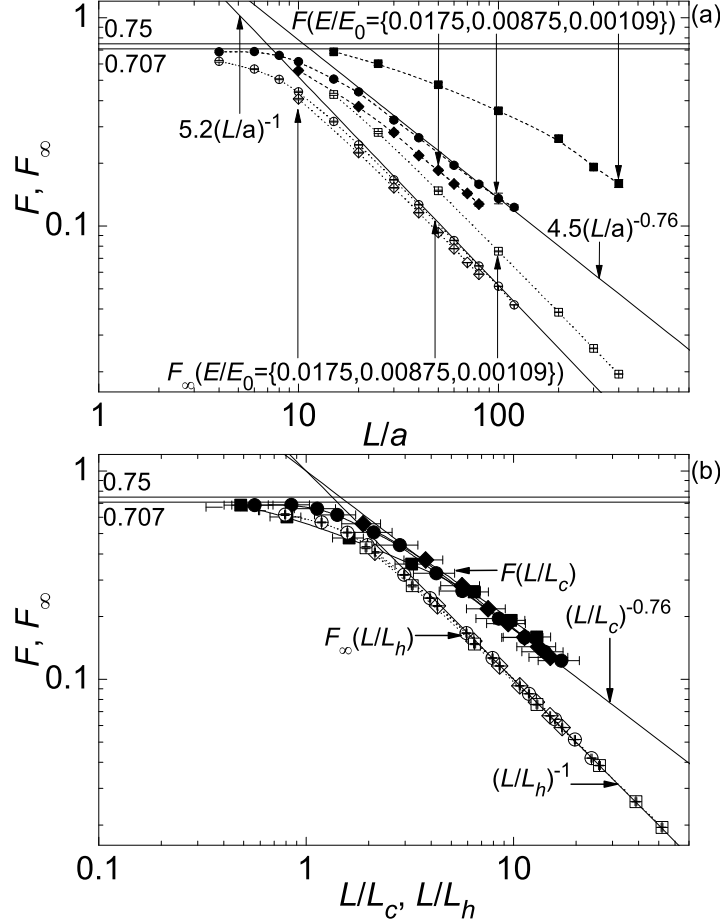


Figure 7. Average Fano factor F and its high-frequency counterpart F_1 as functions of sample length L normalized to: (a) the localization length a , and (b) the scaling lengths L_c (for F) and L_h (for F_1) (see Fig. 8 below), for several values of applied field at $T = 0$ and $W = L_c$. Horizontal lines correspond to the average Fano factor for hopping via one and two localized sites [6, 7]. Straight lines are the best fits to the data, while dashed curves are only guides for the eye.

results for long samples are much more interesting. We have found that they may be reasonably well fitted with a universal dependence

$$F = \frac{L_c}{L} \quad ; \quad L \gg L_c : \quad (21)$$

Here α is a numerical exponent; in the current study we could establish that

$$\alpha = 0.76 \quad 0.08 : \quad (22)$$

Equation (21) and the value for α are compatible with our previous results [9] $\alpha = 0.85 \quad 0.07$ (for the same model, but just one particular value of E) and $\alpha = 0.85 \quad 0.02$ (for nearest neighbor hopping on uniform slanted lattices).

Figure 8 shows the fitting parameter L_c as a function of electric field E . In the variable-range hopping region, it may be fitted with the following law,

$$L_c = Ja \frac{E_0}{E} ; \quad J = 0.04 \quad 0.01; \quad = 0.98 \quad 0.08; \quad (23)$$

This law may be compared with the result of the following arguments. According to the arguments given in Ref. [9], parameter L_c may be interpreted as the average percolation cluster length (up to a constant of the order of 1). The theory of directed percolation [34, 35, 36] gives the following scaling:

$$L_c / hxi \frac{x_c}{jxi x_j}^k : \quad (24)$$

Here hxi is the rms d.s. hop length along the field direction, while x_c is its critical value. According to Ref. [36], the critical index k should be close to 1.73. Due to the exponential nature of the percolation, $jxi \propto x_j^{-a}$, while hxi should follow a field scaling similar to that given by Eq. (12). (Square points in Fig. 8 show that this is true for our simulation results as well.) Thus for sufficiently large hxi we arrive at Eq. (23) with $a = \frac{1}{3} (1 + k) = 0.911$. Equation (24) shows that this value is quite compatible with our numerical result, thus confirming the interpretation of L_c as the average percolation cluster length.

Note that in the variable-range hopping regime, L_c has a different field dependence and is much larger than the average hop length. However, as the applied electric field approaches E_0 , both lengths become comparable with each other and with the localization radius a .

6. Discussion

To summarize, our results for average conductivity and hop statistics are in agreement with the well-known semi-quantitative picture of hopping, including the usual variable-range hopping at low fields ($E \ll E_T$) and "high-field" variable-range hopping at $E_T \ll E \ll E_0$. However, our supercomputer-based simulation has allowed, for the first time, a high-precision quantitative characterization of hopping, for a particular but very natural model. Moreover, our model also describes the "ultra-high field" region ($E \gg E_0$) where the variable-range hopping picture is no longer valid, since from most localized sites an electron can hop, with comparable probability, to several close sites. (In the last region, there are no clearly defined percolation clusters; rather, electrons follow a large number of interwoven trajectories.)

Our simulations of shot noise at 2D hopping have confirmed our earlier hypothesis [9] that in the absence of substantial Coulomb interaction, in sufficiently large samples ($L; W \gg L_c$) the Fano factor F scales approximately proportionally to $1=L$ - see Eq. (21). Other confirmations of this hypothesis have come from recent experiments with lateral transport in SiGe quantum wells [37] and GaAs MESFET channels [38, 39]. Unfortunately, these experiments are not precise enough to distinguish the small difference between the exponent in Eq. (21) from unity.

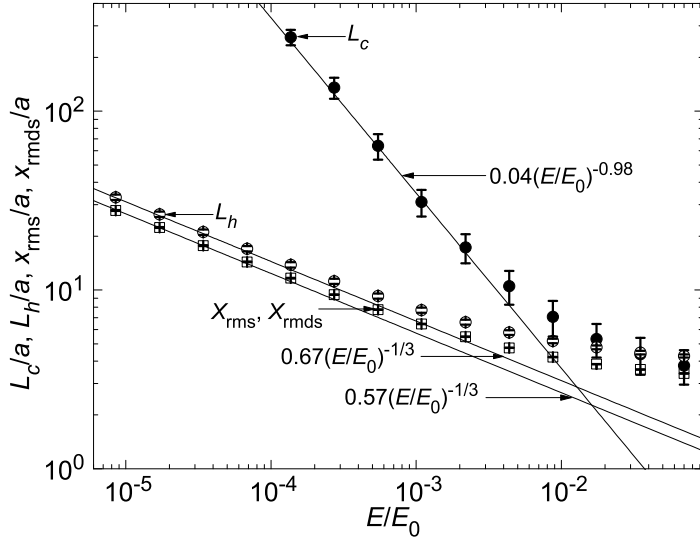


Figure 8. The values of L_h and L_c giving the best fitting of shot noise results by Eqs. (20) and (21) as functions of applied electric field E (open and solid circles, respectively). Open squares show the simple and direction-weighed average hop length along the applied field direction, defined similarly to Eqs. (10) and (11). Straight lines are the best fits to the data.

The hypothesis that γ is in fact equal to 1 for sufficiently long samples seems appealing, because it would mean the simple addition of mutually-independent noise voltages generated by sample sections connected in series. On the contrary, a deviation of γ from unity would mean that dynamical correlations of electron motion in percolation clusters persist even at $L \ll L_c$. We can present, as an example, at least one exactly solvable model (the "asymmetric single exclusion process", or ASEP [40]) in which the dynamical correlations may change from 1 to 0.5. (It is instructive to notice that in the ASEP model the dynamical correlations do not affect average transport characteristics, and may be ignored, in particular, in calculations of dc current.) On the other hand, our results for substantial Coulomb interaction [14] show that in this case γ does in fact approach 1 in sufficiently large conductors.

From the point of view of possible applications in single-electron devices [12], the fact that F may be suppressed to values much less than unity, may seem encouraging, since it enables the use of circuit components with quasi-continuous charge transport for the compensation of random background charge in single-electron islands. However, in order to achieve the really quasi-continuous transfer (say, $F \approx 0.1$), the sample length L has to be at least an order of magnitude longer than the percolation cluster length scale L_c . On the other hand, L_c itself, especially in the most interesting case of low applied fields, is substantially longer than the localization length a (Fig. 8), which is of the order of a few nanometers in most prospective materials, e.g., amorphous silicon. Hence, it

may be hard to implement sub-electron transport in conductors substantially shorter than 100 nm. This size is too large for the most important case of room temperature single-electron circuits [12], because of large stray capacitance that effectively adds up to the capacitance of the island to be serviced.

Acknowledgments

Fruitful discussions with B. Shklovskii and D. Tsigankov are gratefully acknowledged. The work was supported in part by the Engineering Physics Program of the Office of Basic Energy Sciences at the U.S. Department of Energy. We also acknowledge the use of the following supercomputer resources: our group's cluster Njal (purchase and installation funded by DOD's DURIP program via AFOSR), Oak Ridge National Laboratory's IBM SP computer Eagle (funded by the Department of Energy's Office of Science and Energy Efficiency program), and also IBM SP system Tempest at Maui High Performance Computing Center and IBM SP system Haba at NAVO Shared Resource Center. Computer time on two last machines has been granted by DOD's High Performance Computing Modernization Program.

References

- [1] N.F. Mott and J.H. Davies, *Electronic Properties of Non-Crystalline Materials*, 2nd Ed., (Oxford Univ. Press, Oxford, 1979); N.F. Mott, *Conduction in Non-Crystalline Materials*, 2nd Ed. (Clarendon Press, Oxford, 1993).
- [2] B.I. Shklovskii and A.L. Efros, *Electronic Properties of Disordered Semiconductors* (Springer, Berlin, 1984).
- [3] Hopping Transport in Solids, edited by A.L. Efros and M. Pollak (Elsevier, Amsterdam, 1991).
- [4] Ya. Blanter and M. Büttiker, *Phys. Repts.* 336, 2 (2000).
- [5] K.A. Matsuoka and K.K. Likharev, *Phys. Rev. B* 57, 15613 (1998).
- [6] Yu.V. Nazarov and J.J.R. Struben, *Phys. Rev. B* 53, 15466 (1996).
- [7] Y.K. Inkhawala and A.N. Korotkov, *Phys. Rev. B* 62, R7727 (2000).
- [8] A.N. Korotkov and K.K. Likharev, *Phys. Rev. B* 61, 15975 (2000).
- [9] V.A. Sverdlov, A.N. Korotkov, and K.K. Likharev, *Phys. Rev. B* 63, 081302(R) (2001).
- [10] V.A. Sverdlov, Y.A. Inkhawala and A.N. Korotkov, *Preprint cond-mat/0504208*.
- [11] Note that in contrast with some prior publications, we do not include the factor 2 in the exponent. This difference should be kept in mind at the result comparison.
- [12] K. Likharev, *Proc. IEEE* 87, 606 (1999).
- [13] T. Sameshita and S. Uzui, *J. Appl. Phys.* 70, 1281 (1991).
- [14] Y.A. Inkhawala, V.A. Sverdlov and K.K. Likharev, *Preprint cond-mat/0412209* (Submitted to *Journal of Physics: Condensed Matter*).
- [15] N.S. Bakhvalov, G.S. Kazacha, K.K. Likharev, and S.I. Serdyukova, *Sov. Phys. JETP* 68, 581 (1989).
- [16] C.W. Asshauer, *Computational Single-Electronics* (Springer, Berlin, 2001), Ch. 3.
- [17] W. Brügel, G.H. Dohler, and H. Heyszenau, *Phil. Mag.* 27, 1093 (1973).
- [18] A.S. Skal and B.I. Shklovskii, *Fiz. Tverd. Tela* 16, 1820 (1974) [*Sov. Phys. Solid State* 16, 1190 (1974)].
- [19] D.N. Tsigankov and A.L. Efros, *Phys. Rev. Lett.* 88, 176602 (2002).
- [20] For a discussion of this issue, see Sec. 4.2 of Ref. [2].

[21] S. M. Arianer and B. I. Shklovskii, *Phys. Rev. B* **46**, 13100 (1992).

[22] B. I. Shklovskii, *Fiz. Tekh. Poluprovodn.* **6**, 2335 (1972) [*Sov. Phys. Semicond.* **6**, 1964 (1973)].

[23] N. Apsley and H. P. Hughes, *Philos. Mag.* **30**, 963 (1974); **31**, 1327 (1975).

[24] M. Pollack and I. Rieß, *J. Phys. C* **9**, 2339 (1976).

[25] R. Rentzsch, I. S. Shlimak and H. Berger, *Phys. Status Solidi A* **54**, 487 (1979).

[26] M. van der Meer, R. Schuchardt and R. Keiper, *Phys. Status Solidi B* **110**, 571 (1982).

[27] This result emphasizes again that the validity of the master equation approach is very limited, and for most transport characteristics this equation fails to give quantitatively correct results for any region in the $[E; T]$ space.

[28] A. N. Korotkov, D. V. Averin, K. K. Likharev, and S. A. Vasenko, in *Single-Electron Tunneling and Mesoscopic Devices*, edited by H. Koch and H. Luebbig (Springer, Berlin, 1992), p. 45.

[29] A. N. Korotkov, *Phys. Rev. B* **49**, 10381 (1994).

[30] B. I. Shklovskii, *Solid State Commun.* **33**, 273 (1980); Sh. M. Kogan and B. I. Shklovskii, *Sov. Phys. Semicond.* **15**, 605 (1981).

[31] B. I. Shklovskii, *Phys. Rev. B* **67**, 045201 (2003).

[32] In the case of hopping, the noise intensity is not exactly proportional to dc current, because the noise suppression factor depends on the ratio $L=L_c$, where the characteristic length L_c is itself a function of applied electric field, and hence (implicitly) of dc current – see Figs. 7–8 and their discussion below.

[33] D. V. Averin and K. K. Likharev, in *Mesoscopic Phenomena in Solids*, edited by B. L. Altshuler, P. A. Lee, and R. A. Webb (Elsevier, Amsterdam, 1991), p. 173.

[34] D. Stauffer and A. Aharony, *Introduction to Percolation Theory*, Rev. 2nd Ed., (Taylor and Francis Inc, Philadelphia, 1994).

[35] S. P. Obukhov, *Physica A* **101**, 145 (1980).

[36] J. W. Essam, K. DeBell, J. Adler, and F. M. Bhatti, *Phys. Rev. B* **33**, 1982 (1986).

[37] V. V. Kuznetsov, E. E. Mendez, X. Zuo, G. Snider, and E. Crooke, *Phys. Rev. Lett.* **85**, 397 (2000).

[38] S. H. Roshko, S. S. Safronov, A. K. Savchenko, W. R. Tribe, and E. H. Linfield, *Physica E* **12**, 861 (2002).

[39] A. K. Savchenko, S. S. Safronov, S. H. Roshko, D. A. Bagrets, O. N. Jouravlev, Y. V. Nazarov, E. H. Linfield and D. A. Ritchie, *Phys. Stat. Sol. (B)* **241**, No. 1, 26–32 (2004).

[40] B. Derrida, *Phys. Reports* **301**, 65 (1998).